JOURNAL OF COASTAL SCIENCES

Journal homepage: www.jcsonline.co.nr

ISSN: 2348 – 6740 Volume 4 Issue No. 2 - 2017 Pages 9-16

Evaluation of geoelectric parameters to delineate the subsurface fractures for groundwater exploration around coastal Maharashtra, India

N. Suneetha, G. Gupta* and M. Laxminarayana

Indian Institute of Geomagnetism, New Panvel (W), Navi Mumbai 410218–India

A B S T R A C T

Modelling of electrical resistivity data especially from coastal area assumes an explicit significance for groundwater prospecting studies. Direct current (DC) Vertical electrical sounding (VES) data were acquired from 84 locations around Aronda-Redi-Vengurla-Malvan region, Sindhudurg district, Maharashtra, India, with an objective to decipher the structural trend for identifying groundwater potential zones of the area using geophysical indicators. The VES curves obtained were primarily of 3-5 geoelectric layers. One-dimensional inversion results divulge that the top layer is predominantly comprised of laterites/fractured laterites followed by an assortment of clay/clayey sand and granulites/fractured granulites as basement rocks. Several NNE-SSW and NW-SE oriented major lineaments and its criss-crosses have been reported in this region and the source of groundwater appears to be contained in weathered/semi-weathered layer of laterite/clayey sand at depth of 10-12 m from the surface. Geoelectric parameters for interpretation included curve type, anisotropy coefficient, fracture porosity, and reflection coefficient. The electrical anisotropy varied from 1 to 3.95, while the reflection coefficients ranged from 0.1 to 0.99 in the study area. It is seen that stations with low reflection coefficient revealed higher electrical anisotropy, suggesting an inverse correlation between these two parameters. The northeastern, southern and northwestern part of the study area revealed higher values of fracture porosities, wherein a positive relationship with the high and low values of electrical anisotropy was observed. These results would be helpful for interpreting the geological signatures like fractures, joints and lineaments for identifying groundwater prospective zones in the coastal area.

A R T I C L E I N F O

Received
21 March 2017
Accepted
28 October 2017
Available online
28 November 2017

Keywords
Electrical resistivity
Inversion
Geophysics
Anisotropy
Schlumberger
sounding

*Corresponding author, E-mail address: **ggupta@iigs.iigm.res.in**
Phone: +919820387080
© 2017 – Journal of Coastal Sciences. All rights reserved

1. Introduction

Groundwater is an integral part of the environment, and therefore cannot be looked upon in isolation. Being a key source for drinking and domestic needs, its evaluation assumes an enormous consequence to people living in the coastal regions around the world. Nowadays scarcity of this precious natural resource is more because of limited amount available and over exploitation. Further socio-economic and climate factors are expected to play a major role in groundwater prospecting in semi-arid crystalline hard area. In a crystalline hard rock terrain, groundwater usually occurs in the weathered basement and the fractured rocks (Verma et al., 1980). Fractured basement that is sandwiched between the overburden and bedrock often contains significant amount of water (Batte et al., 2008). The existence of weathered and fractured granulites and granites, coupled with weathered zones may augment the probability of high yielding boreholes. The present study area is located in Sindhudurg district, western Maharashtra, India where sand and gravel aquifers which are favourable for constructing high-yielding wells are scare (Fig. 1a). In the overburden, the aquifers are mainly composed of clayey sand. Shear zones are expected at several places in the study area (Deshpande 1998), where the exposed basement is fractured. The fractured and shear zones are likely to be potential proxy indicators for groundwater prospecting. Therefore, the delineation of geologically weaker zones such as fractures is of significant societal importance. Furthermore, the groundwater level fluctuates in response to tidal variation in the vicinity of the coastal region adjacent to the Arabian Sea. As a result, there is always a possibility of saltwater intrusion in fresh water pockets in the coastal belt of Maharashtra, which leads to the pollution of groundwater (Song et al., 2007; Mondal et al., 2013; Maiti et al., 2013a, Srinivas et al., 2014) and hence should be monitored periodically. Modelling and interpretation of Direct Current (DC) resistivity sounding in the region would play chief role in elucidating the above patterns.

The Direct Current (DC) vertical electrical sounding (VES) method has been employed widely to solve numerous geophysical problems (Zohdy et al., 1974; Gupta et al., 2014). Here, current is introduced directly into the ground through a pair of current electrodes and the ensuing potential variation is measured between a pair of potential electrodes. This technique provides the apparent resistivity distribution against depth. The depth of penetration of electrical signal is usually about one-third of the distance between the electrode separations. The relation between the observed apparent resistivity and model parameters i.e., true resistivity and layer thickness being non-linear, forward numerical models are commonly used to relate the measured/observed data to desired model parameters. Inverse modelling starts with initial data specifying a starting model, and it estimates model parameters by minimizing a specific error/misfit function of the data and model parameters (Menke 1984).

In the present work, VES data from all the 84 stations have been analysed using secondary geophysical indicators like longitudinal conductance, transverse resistance, electrical anisotropy, fracture porosity and electrical reflection coefficient in order to delineate the subsurface fractures which might be favourable zones for groundwater exploration.

2. Study area

The study area is located between the latitude 15.75° to 16.15° N and longitude 73.5° to 73.80° E. It is bordered by the Arabian Sea on the west and Sahyadri ranges to the eastern side while the Karli River passes through the study area. The geological map of the study region is shown in Fig.1a. The entire region is characterised by a typical physiographic set-up with undulating terrain, except in coastal plains and exhibits a dendritic drainage pattern (Gupta et al., 2014). The climatic conditions in the area are strongly influenced by its geographical conditions, which fall under the 'Assured and High Rainfall zone'. The winter season is from December to February with mean daily maximum temperature at 32.7°C and the mean daily minimum temperature at 18.7°C, followed by summer from March to May. The southwest monsoon persists during June to September, while, October and November comprise the post-monsoon season. Very high relative humidity ranging from 86% to 90% is experienced during the southwest monsoon, whereas during winter and summer months it is about 57% (Paranjape 2009). The annual rainfall over the entire district varies from 2300 mm to about 3205 mm. While the western part of the district along the coast experiences minimum annual rainfall, it progressively increases towards east and reaches maximum along Western Ghats. The annual rainfall is 3287 mm in Sindhudurg district (Paranjape 2009). The study area exhibits rocks ranging in age from Archaean to Quaternary period. The southern part of the Sindhudurg district near Vengurla and Sawantwadi are characterized by medium to coarse-grained granite gneiss (Archaeans). The Dharwar supergroup overlie the Archaeans and occupy major part of the area comprising psammatic meta-sediments consisting of meta-gabbro, quartz chromites, amphibolites schist and ferruginous phyllite. The general geologic sequence observed in Sindhudurg district is given in Table 1.

Table 1. General geological succession in Sindhudurg district, Western Maharashtra, India (Source: Paranjape 2009, CGWB report)

Geological time	Formation
Recent to sub recent	Alluvium beach sand
Pleistocene	Laterite and lateritic spread
Miocene	Shale with peat and pyrite nodules
Cretaceous to Eocene	Deccan trap basalt lava flows
Upper Pre-Cambrian	Kaladgi series, quartzite, sandstone, shale, and associated limestone
Dharwar Super Group	Phyllite, conglomerate, quartzite

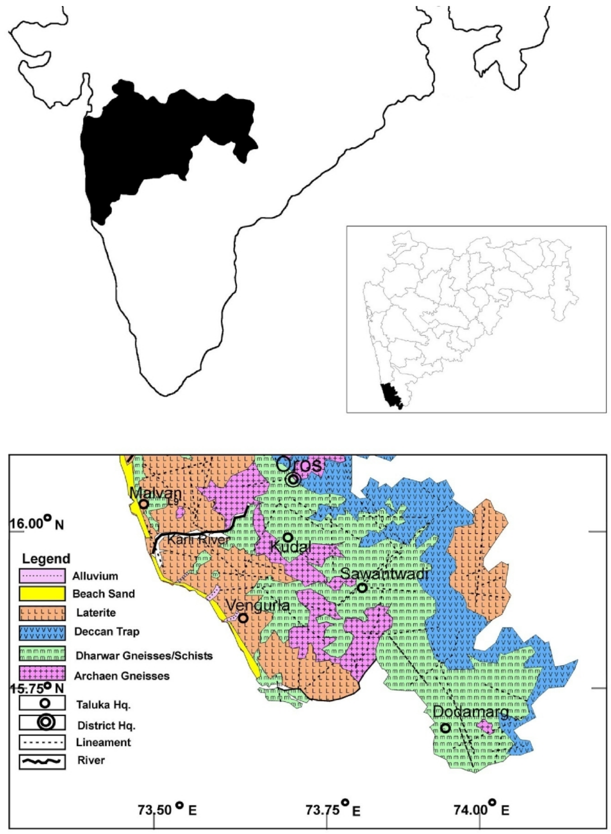

a

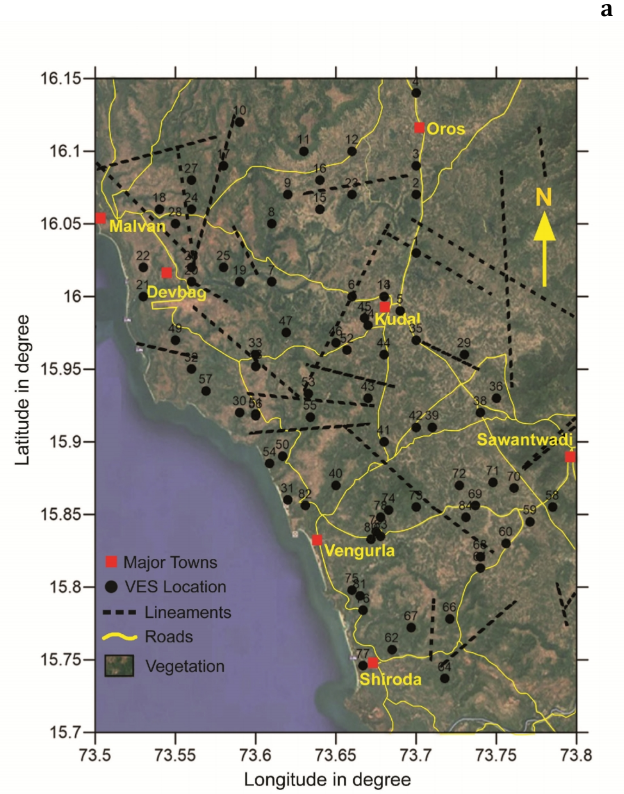

b

Fig.1. **(a)** Geological and tectonic map of the study area. **(b)** Vertical electrical sounding station locations. Also shown are the lineaments, landmarks, major roads and vegetation (Redrawn after GSI 2000).

Dharwarian meta-sediments (Achaean), Kaladgi formation (Precambrian), Deccan Trap lava flows (Upper Cretaceous to lower Eocene), laterites (Pleistocene) and Alluvial deposits (Recent to sub-recent) are the water bearing formation observed in the district. Kaladgi formation is revealed in very limited patches and it is not a potential aquifer, while the alluviums have limited areal coverage essentially along the coast (Paranjape 2009). Primary porosity and permeability are negligent in Dharwarian gneiss/schists and therefore, secondary porosity due to jointing and fracturing plays a major role in groundwater circulation. Laterites being more porous than the Deccan trap basalt thereby form several potential aquifers in the area. Groundwater level in the study area ranges from 2 m to 20 m (Paranjape 2009). Shallow water levels within 10 m below ground level (bgl) are seen in almost entire district during pre-monsoon season. The deeper water levels varying from 10-20 m bgl are observed in northwestern part of the district. Spatial variation of water levels is about 5 m bgl in the entire district during post-monsoon season.

3. Materials and methods

The present resistivity survey encompasses parts of Aronda-Redi-Vengurla-Malvan, Konkan region (Fig. 1b). Data were acquired with Schlumberger electrode configuration at 84 sites using IGIS made SSR-MP-AT instrument, with maximum current electrode spread (AB) of 200 m. Due to the limitations on the logistics set by the rugged topography, the sites were selected on the basis of availability and accessibility. The resistivity meter performed a minimum stack of three measurements for each data point in order to improve the data quality. The field data was processed and modelled using IPI2win inversion software (Bobachev 2003). One-dimensional inversion results of a few representative VES curves are shown in figure 2a-d. The root mean square (RMS) errors vary from 0.31–1.9%. The inferred true electrical resistivity section against depth is also shown along with borehole lithology (to be discussed later) in the area (Fig. 2a-d). The sounding curves on log-log graph suggest 3-5 layered structure in the study area (Orellana and Mooney 1966; Keller and Frischknecht 1966). The resistivity and thickness values thus generated provided the primary parameters, which were used to establish the secondary geoelectric indicators like transverse resistance (T), longitudinal conductance (S) and coefficient of anisotropy (λ), which helps in interpreting the subsurface lithological and structural characteristics with reduced uncertainty (Maillet 1947).

Total longitudinal conductance (S) is defined as,

$$S = \sum_{i=1}^{n} \frac{h_i}{\rho_i} \tag{1}$$

Similarly, the total transverse unit resistance (T) is defined as,

$$T = \sum_{i=1}^{n} h_i \rho_i \tag{2}$$

Where (ρi) and (hi) are the resistivity and thickness respectively and the subscript i indicates the position of the layer in the section. Using eq. (1), the longitudinal resistivity of the current flowing parallel to the layers is given by,

$$\rho_l = \frac{H}{S} = \frac{\sum_{i=1}^{n} h_i}{\sum_{i=1}^{n} \frac{h_i}{\rho_i}} \tag{3}$$

Where H is the depth to the bottom most geoelectric layer. Similarly, the transverse resistivity of the current flowing perpendicular to the layers is expressed using eq. (2) as,

$$\rho_t = \frac{T}{H} = \frac{\sum_{i=1}^{n} h_i \rho_i}{\sum_{i=1}^{n} h_i} \tag{4}$$

The longitudinal resistivity (ρl) is generally less than the transverse resistivity (ρt), unless the medium is uniform (Flathe 1955). Further, Keller (1982) suggested that ρl is dominated by the more conductive layers (in the present case, clay and weathered/fractured basalts) whereas ρt increases rapidly even if a small fraction of resistive layers are present.

Combining eq. (3) and (4), the coefficient of anisotropy (λ) is given by,

$$\lambda = \sqrt{\rho_t / \rho_l} \tag{5}$$

Fracture porosities linked with tectonic fracturing of rocks were estimated using the expression derived by Lane et al., (1995); Kumar et al., (2014),

$$\varphi_f = \frac{3.41 \times 10^4 (N-1)(N^2-1)}{N^2 C(\rho_{max} - \rho_{min})} \tag{6}$$

where φf is the fracture porosity; N is the vertical anisotropy related to the coefficient of electrical anisotropy λ, here the vertical anisotropy is equal to the coefficient of anisotropy (λ), since for Schlumberger 1-D data, both (λ) and N are equal; ρ_{max} and ρ_{min} is the maximum and minimum apparent resistivity (Ω-m) respectively; while C is the specific conductance of groundwater in $\mu s/cm$, which is averaged to 421 $\mu s/cm$ from bore wells and dug wells of the study area.

Here the secondary geophysical indices, namely T, S, ρ_l, ρ_t, λ and φ_f were evaluated at all the 84 VES sites so as to study the anisotropic nature and fracture geometry in the trap covered hard rock terrain for groundwater exploration. Kumar et al., (2014) suggested that high values of λ indicate different degrees of fracturing, with better water-holding ability in hard rock areas. Several workers reported that reflection coefficient (r) reveals the degree of fracturing of the underlying basement (Olayinka 1996; Olasehinde and Bayewu 2011; Bayewu et al., 2014; Vijay Kumar et al., 2015). Olayinka (1996) further suggested that a low value of reflection coefficient exhibits a weathered or fractured basement rock, and therefore has a higher water potential. Thus, the reflection coefficient (r) was calculated as,

$$r = (\rho_n - \rho_{(n-1)})/(\rho_n + \rho_{(n-1)}) \tag{7}$$

where ρ_n is the layer resistivity of the nth layer and $\rho_{(n-1)}$ is the layer resistivity overlying the nth layer.

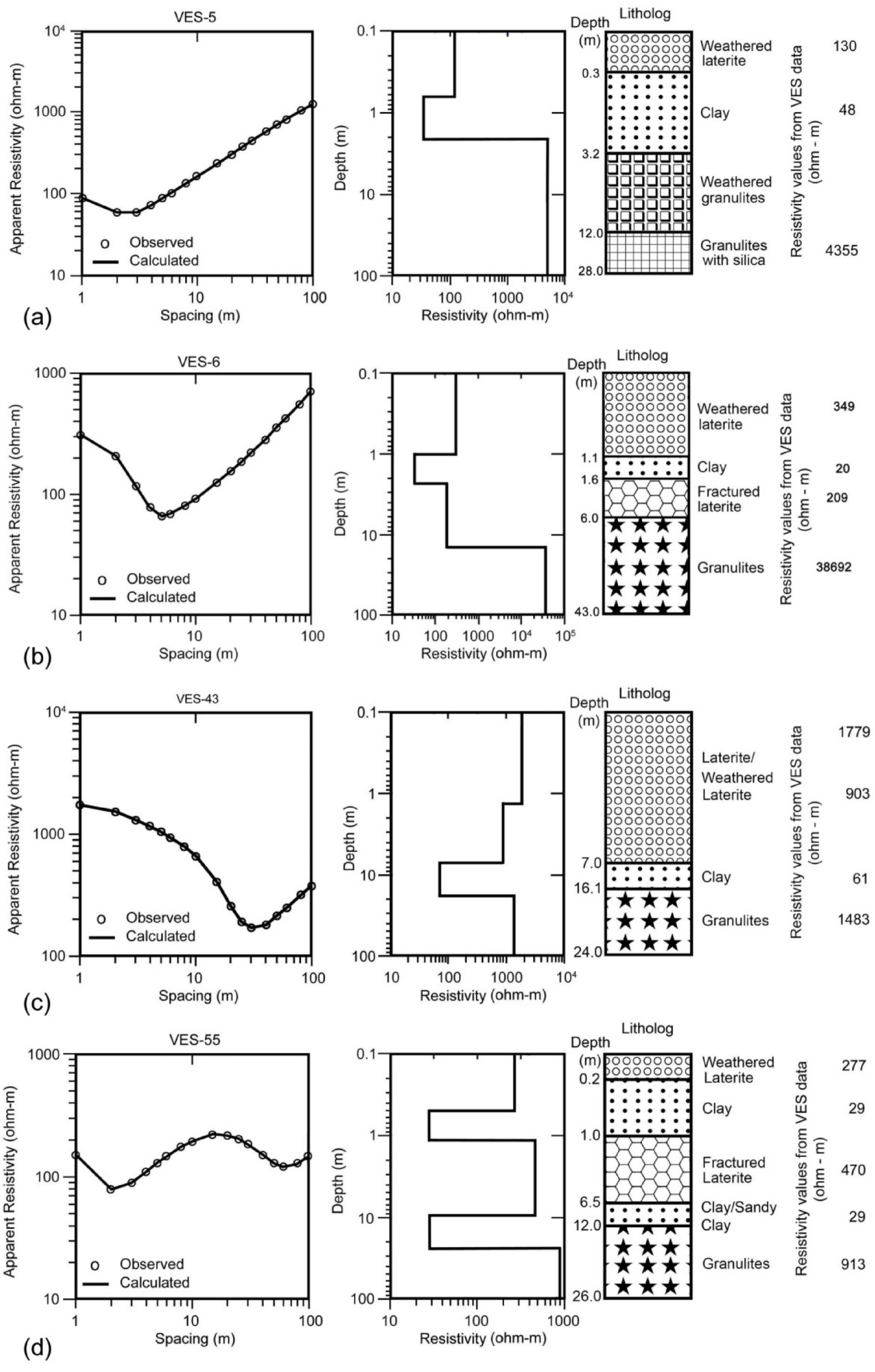

Fig. 2. Vertical electrical sounding curves and inversion results at **(a)** VES 5 **(b)** VES 6 **(c)** VES 43 **(d)** VES 55. Also, the correlation of borehole lithology with the corresponding resistivity values obtained from VES data is shown.

Different data driven interpolation schemes have been developed to generate accurate and representative spatial variation maps (Webster and Oliver 2001; Koehler and Peter 2013). In this study however, kriging interpolation technique via SURFER version 11 is used to calculate the spatial variation of the geoelectric parameters. Kriging is a geo-statistical method based on the linear and unbiased conception of mapping that uses semi-variogram model fitting techniques. It calculates a value at a point of a region of a known semi-variogram without prior information of the distribution mean. Ordinary kriging not only presumes the mean to be constant over the entire area, but also it is assumed to be constant in the local neighbourhood of each estimation point (Bohling 2005).

4. Results and discussion

The longitudinal conductance (S) value ranges between 0.01 to 28 Ω^{-1} in the study area, which helps to differentiate changes in the total thickness of low resistivity materials (Galin 1979). This parameter reveals the disparity of the highly resistive basement topography, implying that high S values are indicative of deeper basement and vice versa (Murali and Patangay 2006; Oteri 1981). Also, if the geologic sequence and clayey overburden is moderately thick, then high longitudinal conductance is suggestive of better protective capacity of aquifers (Oladapo and Akintorinwa 2007). The transverse resistance (T) value varies from a minimum of 11 Ωm^2 to a maximum of 46000 Ωm^2 in the entire study area. Larger T values are associated with zones of high transmissivity and, hence highly permeable to fluid movement. The transverse resistivity in the area varies from 0.6 to 1812 Ωm while the longitudinal resistivity ranges from 0.6 to 682 Ωm. In heterogeneous medium, the transverse resistivity is usually more than the longitudinal resistivity Flathe (1955), but for the medium is homogeneous. This suggests that the current flow and average hydraulic conduction along the longitudinal boundary are greater than those normal to the boundary plane (Ayolabi et al., 2010). Further, Keller (1982) was of the view that longitudinal resistivity is subjugated by the more conductive layers (in the present case, clay and weathered/fractured basalts) whereas transverse resistivity increases quickly even if a small fraction of resistive layers are present. The coefficient of electrical anisotropy (λ) is evaluated based on longitudinal resistivity and transverse resistivity. The value of λ ranges from 1 to 3.9 in the study area. The coefficient of anisotropy is generally 1 and rarely exceeds 2 in most of the geological settings (Zohdy et al., 1974). If the λ value varies between ~1 and up to 1.5, it is considered to be a prospective groundwater zone. Therefore, low λ values are associated with lowest water table fluctuation and high λ values are related to higher water table fluctuation in the region.

The coefficient of anisotropy (Fig. 3a) shows an increasing trend from NE to SW direction with high λ value (>2) at the VES stations 1, 43, 55, 50 and 54. A conspicuous NW-SE oriented high λ value (> 1.7) is also revealed at VES stations 18, 26, 20, 7, 47, 40, 84, 68 and 67 (Fig. 3a). This indicates the heterogeneous and anisotropic nature of the subsurface in both NE-SW and NW-SE directions. These stretches are therefore more fractured in the study area suggesting moderately enhanced potential groundwater zone. The fracture porosity (φ_f) values divulge higher porosities on the northeastern, southern and northwestern part of the study area (Fig. 3b). A maximum porosity value of 0.6 was observed in the southern part at VES 62, while VES 20 and 26 in the northwestern part revealed porosity values in the range 0.4-0.5%. Porosity value of 0.1 was observed at VES 1 in the northeastern part. Minimum porosity value of 0.0000004 (VES 31 and 33) were obtained at western part.

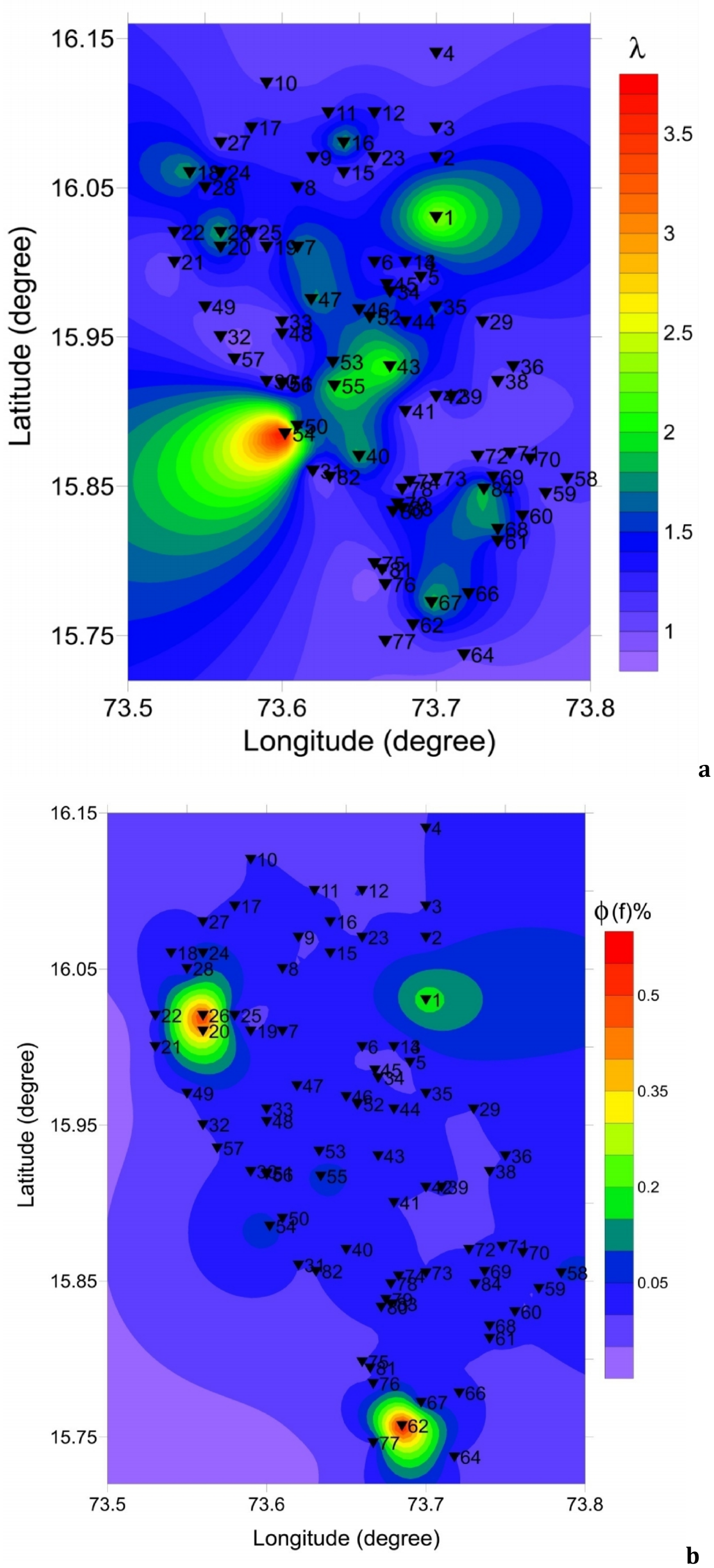

Fig. 3. **(a)** Spatial variation of electrical anisotropy (λ) in the study area. **(b)** Spatial variation of the fracture porosity map in the study area.

There is a fairly good positive correlation between the fracture porosity values with the high and low values of electrical anisotropy (λ). As stated earlier, the anisotropy values show an increasing trend in NE-SW as well as in NW-SE directions, suggesting diverse degree of fracturing in multi direction. This means that the fractured rocks are likely to possess water with superior water retention ability resulting in higher porosity values (Niwas and Celik 2012).

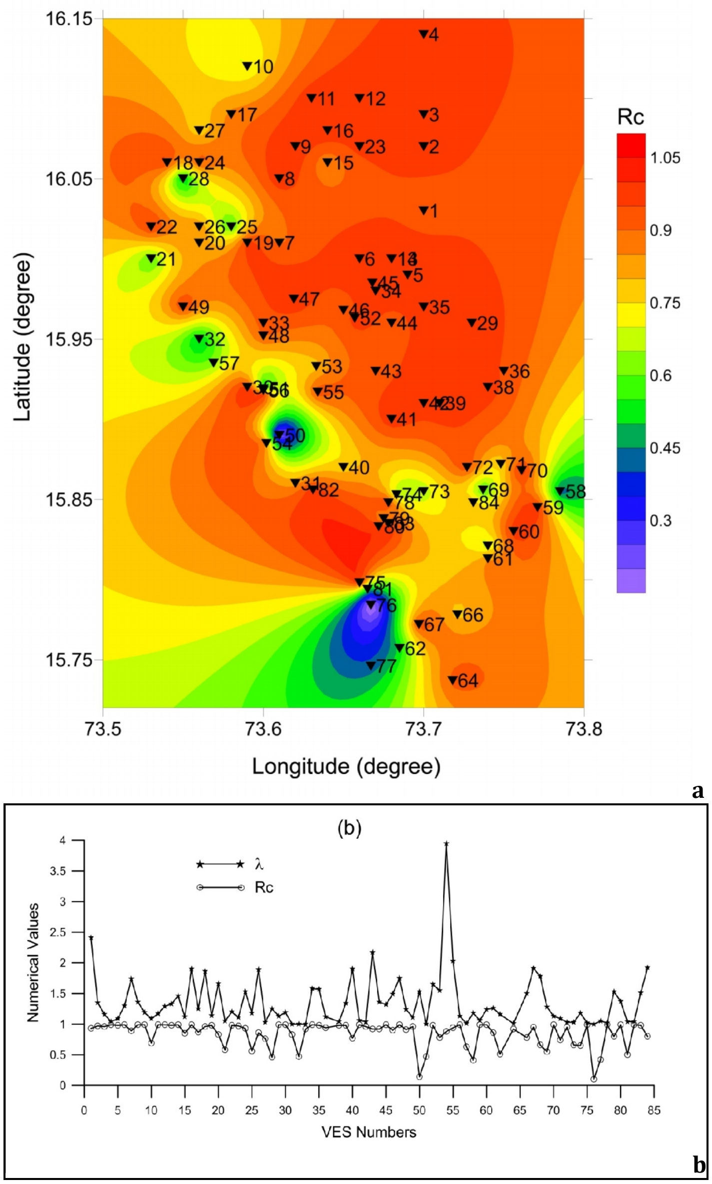

Fig. 4. (a) Spatial variation of reflection coefficient in the study area. **(b)** Plot of coefficient of anisotropy (λ) and reflection coefficient (Rc) with VES number.

As mentioned earlier, the reflection coefficient (Rc) can reveal an idea about the aquiferous nature of the basement rocks thereby indicating areas of high density water filled fractures. The reflection coefficient map (Fig. 4a) suggests that Rc values less than 0.9 may reveal weathered or fractured rocks, and therefore, may have a high water potential. A prominent low is revealed in the NW-SE orientation wherein, VES stations 10, 28, 25, 21, 32, 57, 51, 50, 73, 74, 69, 76, 77 divulge Rc values in the range 0.1-0.69. This NW-SE trend also follows λ high along a lineament discussed earlier. The NE-SW lineament, depicted as high λ value, is feebly observed at VES station 43, 55, 50 and 54 where the Rc values are 0.94-0.88. It is also seen that areas with low reflection coefficient values correspond to high λ values. Thus, it may be surmised that lower reflection coefficient values is observed where the electrical anisotropy is high, suggesting an inverse relationship between these two indices (Fig. 4b). This also advocates that fractures in the basement rocks have a higher groundwater prospect.

4.1. Assessment of groundwater potential

LANDSAT imageries study in Sindhudurg district revealed numerous NNW-SSE to NE-SW oriented lineaments (Sarkar and Soman 1986). Several parallel en echelon lineaments trending NE-SW and NNW-SSE runs from Malvan in the north to Nivti and Math in the south near the coast (GSI 2000). These lineaments are linked with intense fracturing. Two-dimensional modelling of resistivity profiles in parts of the present study area (Maiti et al., 2013b) observed that the groundwater flow is partly controlled by existing lineaments, fractures, and major joints. Several NE-SW lineaments and a NNW-SSE mega lineament have been reported from remotely sensed data in this region that controls the physical setting of the coast (Hanamgond and Mitra 2008). Narain et al., (1968) and Sarkar and Soman (1983) are of the view that rejuvenation of these faults and lineaments during different time periods as is evidenced from the brecciated Dharwarian quartzite and emplacement of silica veins in the Kaladgi sandstones and a decrease of a few tens of meters in altitude of laterite along the major lineaments. These also point to the tectonic movement associated with the west coast faulting in this and adjoining areas (Powar 1993).

The primary porosity is negligent in the Deccan trap basalts (Deolankar 1980) and therefore the secondary porosity due to jointing and fracturing plays a critical role in groundwater circulation. As mentioned earlier, groundwater occurs under unconfined conditions in the phreatic zone up to a depth of about 15 m in the weathered zone, fractures and joints in the massive unit and weathered/fractured vesicular units. It is further reported that the aggregate porosity of weathered basalt is about 34% in Deccan Volcanic Province, whereas the specific yield is only about 7% (Deolankar 1980). The high porosity and the low specific yield imply higher specific retention in weathered basalt. This is likely to be caused due to the presence of clay minerals in the weathered basalt, which has higher water withholding ability.

As mentioned earlier, Sindhudurg district of Maharashtra is covered by Deccan volcanic rocks and most of the soils are derived from lateritic rocks. Groundwater flows preferentially through a network of voids, joints, and fractures and thus monitoring the shallow distribution of the resistivity patterns in the area is imperative for mapping faults, fractures, joints, preferential groundwater conduits, and lineaments affecting groundwater circulation patterns. This region is in proximity to the Arabian Sea and therefore groundwater level varies in response to tidal changes. The fresh groundwater is thus contaminated by salt water, which displaces or mixes with freshwater. As a consequence, the near surface distribution pattern of electrical properties is altered (Todd 1980).

The apparent resistivity maps obtained for half-electrode spacing (AB/2) of 2, 5, 15 and 20 are given in Fig. 5a, b, c and d respectively. The study area exhibits analogous characteristics from surface up to depth of 20 m as shown in Fig 5a-d. The NW, SE and central parts of the study area reveals high resistive terrain at the surface (Fig. 5a). The resistive feature is presumably due to the presence of widespread lateritic exposure in the study area. The SW and western parts of the study area, adjoining the Arabian Sea, reveals low resistivity, which is due to the effect of saline water intrusion from the Arabian Sea into the inland. The apparent resistivity surface maps further suggests two major groups of NW–SE and NE–SW oriented lineaments as shown in Fig. 5a. The NE–SW lineament passing through VES stations 18, 28, 24, 9 and 16 is parallel to the course of Karli River. As can be seen from Fig. 5a, few lineaments are criss-crossed and the intersection points of these lineaments are likely to be most favourable zone for fresh groundwater recharge in the area. It is pertinent to mention here that the NNW-SSE and NE-SW trending lineaments delineated by Sarkar and Soman (1986) and GSI (2000) are also observed in the apparent resistivity surface maps (Fig. 5a).

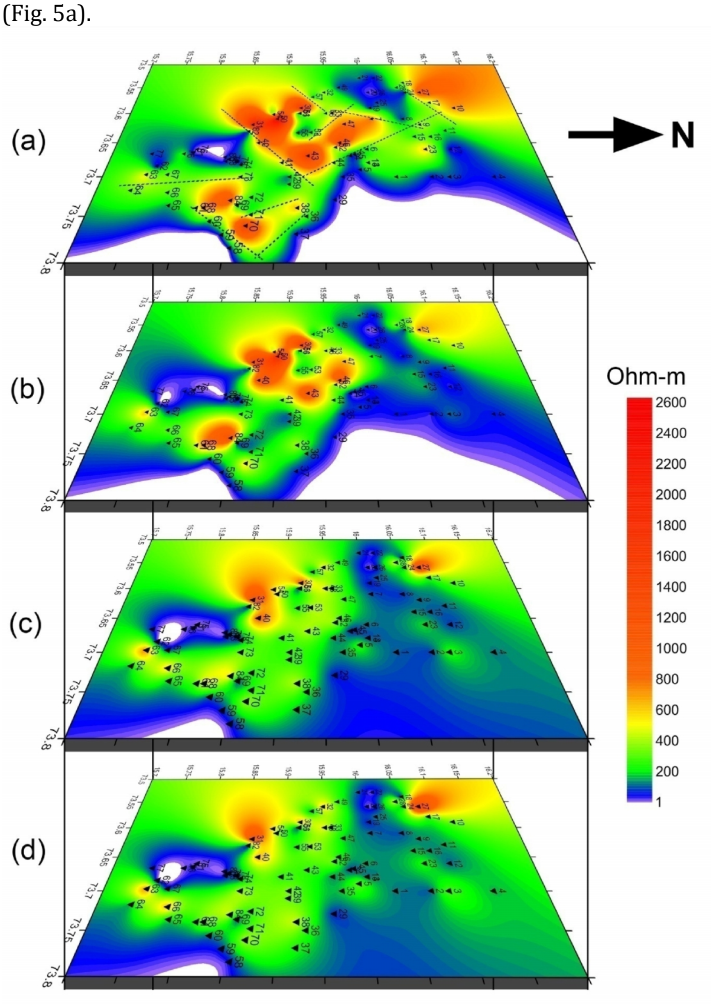

Fig. 5. Apparent resistivity surface map at different depths **(a)** at depth = 2 m **(b)** at depth = 5 m **(c)** at depth = 15 m **(d)** at depth = 20 m

In general, the inverted results of VES have been found to be compatible with the borehole lithology of the study area (Fig. 2a-d), wherein, the correlation between borehole logs consisting of four to five different types of geological formations together with the deduced true resistivity values obtained from VES data is shown. However, some discrepancies are observed in the number of layers obtained from the borehole log and VES data, which is primarily due to the large resistivity contrast between bedrock and regolith. These may result in suppression of intermediate fractured resistivity layers containing considerable quantities of water, stumbled upon during drilling (Ghosh 1971). The entire study area, as revealed from the lithologs, suggest that the top layer consists of laterite soil followed by clay. This is underlain by fractured laterite with granulites as the bedrock. The aquifer structure in the study area is partially composed of clayey sand, fractured laterites and weathered granulites.

5. Conclusion

Groundwater typically occurs in discrete aquifers in geologically intricate region and thus delineating the potential aquifer zones is often a tedious task. In the present study, vertical electrical sounding (VES) data from 84 locations located around Aronda-Redi-Vengurla-Malvan region in Sindhudurg district, Maharashtra has been acquired with an objective to reveal the sub-surface structural features for identifying groundwater potential zones using secondary geophysical indicators. The inversion results of 84 VES data reveal that the top layer predominantly comprises of laterites followed by assortment of clay/ clayey sand and garnulites as basement rocks. The source of groundwater seems to exist in weathered/semi-weathered/fractured layer of laterite/clayey sand/granulites within the depth of 10–15 m from the surface and the true electrical resistivity corroborates fairly well with the borehole lithology in the area. Further, the apparent resistivity spatial variation maps at different depths could identify the NW–SE and NE-SW oriented major lineaments and its criss-crosses, which also forms potential locale of groundwater. The coefficient of electrical anisotropy (λ) varied from 1 to 3.9 in the study area with an increasing trend from NE to SW and NW to SE directions. This reflects the fact that the subsurface in both these directions are heterogeneous and anisotropic in nature and hence more fractured, suggesting reasonably better prospective groundwater zone. A positive relationship between the fracture porosity values with the high and low values of electrical anisotropy is revealed suggesting that the fractured rocks with better water retention capacity ensures higher porosity values. Reflection coefficient values suggest a low (0.1-0.69) in the NW-SE orientation following the high λ. However, the high λ value in the NE-SW lineament is weakly seen in the reflection coefficient map with values between 0.94-0.88. Apparently, it is noticed that areas with low reflection coefficient values correspond to high λ values, signifying an inverse relationship between these two indices. It is therefore envisaged that the present results will proffer reliable information for a comprehensive groundwater development in Sindhudurg district and adjoining coastal areas.

Acknowledgment

The authors are grateful to Dr. D.S. Ramesh, Director, Indian Institute of Geomagnetism, New Panvel for the motivation and kind consent to publish the work. The authors express their deep sense of thankfulness to Shri B.I. Panchal for drafting and re-drawing the figures.

References

Ayolabi, E.A., Folorunso, A.F., and Oloruntola, M.O., 2010. Constraining causes of structural failure using Electrical Resistivty Tomography (ERT): A case study of Lagos, Southwestern, Nigeria. Mineral Wealth, 156: 7-18.

Batte, A.G., Muwanga, A., Sigrist, P.W., and Owor, M., 2008. Vertical electrical sounding as an exploration technique to improve on the certainty of groundwater yield in the fractured crystalline basement aquifers of eastern Uganda. Hydrogeol. Jour., 16: 1683–1693.

Bayewu, O.O., Oloruntola, M.O., Mosuro, G.O., Folorunso, I.O., and Kolawole, A., 2014. Evaluation of Resistivity Anisotropy of parts of Ijebo Igbo, Southwestern, Nigeria Using Azimuthal Resistivity Survey (ARS) Method. Jour. Geography Geology, 6(4): 140-150.

Bobachev, A., 2003. *Resistivity Sounding Interpretation*; IPI2WIN: Version 3.0.1, a 7.01.03, Moscow State University.

Bohling, G., 2005. Introduction to Geostatistics and Variogram Analysis. Kansas Geological Survey: Lawrence, KS, USA, pp. 1–20.

Deolankar, S.B., 1980. The Deccan Basalt of Maharashtra, India- their potential as aquifers. Ground Water, 18(5): 434-437.

Deshpande, G.G., 1998. Geology of Maharashtra. Geological Society of India, Bangalore, 223p.

Flathe, H., 1955. Possibilities and limitations in applying geoelectrical methods to hydrogeological problems in the coastal area of northwest Germany. Geophysical Prospecting, 3: 95–110.

Galin, D.L., 1979. Use of longitudinal conductance in vertical electrical sounding induced potential method for solving hydrogeologic problems. Vestrik Moskovskogo University Geology, 34: 74–100.

Ghosh, D., 1971. The application of linear filter theory on the direct interpretation of geoelectrical resistivity sounding measurements. Geophysical Prospecting, 19: 192–217.

GSI, 2000. Seismotectonic atlas of India and its environs. Geological Survey of India publication, 87p.

Gupta, G., Maiti, S., and Erram, V.C., 2014. Analysis of electrical resistivity data in resolving the saline and fresh water aquifers in west coast Maharashtra, India. Jour. Geol. Soc. India, 84: 555-568.

Hanamgond, P.T., and Mitra, D., 2008. Evolution of Malvan coast, Konkan, west coast of India- A case study using remote sensing data. Jour. Coastal Res., 24(3): 672-678.

Keller, G.V., 1982. Electrical Properties of Rocks and Minerals. In: Carmichael, R.S. (ed.), Hand Book of Physical Properties of Rocks. CRC Press, pp. 217-293.

Keller, G.V., and Frischknecht, F.C., 1966. Electrical methods in geophysical prospecting. Oxford, Pergamon Press Inc.

Koehler, K.A. and Peters, T., 2013. Influence of analysis methods on interpretation of hazard maps. Ann. Occup. Hyg., 57(5): 558-570.

Kumar, D., Rai, S.N., Thiagarajan, S., and Ratnakumari, Y., 2014. Evaluation of heterogeneous aquifers in hard rocks from resistivity sounding data in parts of Kalmeshwar taluk of Nagpur district, India. Curr. Science, 107(7): 1137-1145.

Lane, Jr. J.W., Haeni, F.P., and Watson, W.M., 1995. Use of a square array direct current resistivity method to detect fractures in crystalline bedrock in New Hampshire. Ground Water, 33(3): 476–485.

Maiti, S., Erram, V.C., Gupta, G., Tiwari, R.K., Kulkarni, U.D., and Sangpal, R.R., 2013a. Assessment of groundwater quality: A fusion of geochemical and geophysical information via Bayesian Neural Networks. Environ. Monit. Assessment, 185: 3445-3465.

Maiti, S., Gupta, G., Erram, V.C., and Tiwari, R.K., 2013b. Delineation of shallow resistivity structure around Malvan, Konkan region, Maharashtra by neural network inversion of vertical electrical sounding measurements. Environ. Earth Science, 68: 779-794.

Maillet, R., 1947. The fundamental equation of electrical prospecting. Geophysics, 12: 529–556.

Menke, W., 1984. Geophysical data analysis: discrete inverse theory. New York Academic.

Mondal, N.C., Singh, V.P., and Ahmed, S., 2013. Delineating shallow saline groundwater zones from Southern India using geophysical indicators. Environ. Monit. Assessment, 185: 4869-4886.

Murali, S., and Patangay, N.S., 2006. Principles of Application of Groundwater Geophysics. 4th ed., India Association of Geophysicists, Hyderabad.

Narain, H., Kaila, K.L., and Verma, R.K., 1968. Continental margins of India. Canadian Jour. Earth Sci., 5: 1961-1965.

Niwas, S., and Celik, M., 2012. Equation estimation of porosity and hydraulic conductivity of Ruhrtal aquifer in Germany using near surface geophysics. Jour. Appl. Geophys., 84: 77–85.

Oladapo, M.I., and Akintorinwa, O.J., 2007. Hydrogeophysical study of Ogbese Southwestern, Nigeria. Global Journal of Pure and Applied Science, 13(1): 55-61.

Olasehinde, P.I., and Bayewu, O.O., 2011. Evaluation of electrical resistivity anisotropy in geological mapping: A case study of Odo Ara, West Central Nigeria. African Journal of Environmental Science and Technology, 5(7): 553-566.

Olayinka, A.I., 1996. Non Uniqueness in the Interpretation of Bedrock Resistivity from Sounding Curves and its Hydrological Implications. Water Resour. Jour. NAH, 7(1-2): 55-60.

Orellana, E., and Mooney, H.M., 1966. Master Tables and Curves for Vertical Electrical Sounding over Layered Structures. Interciencia, Madrid, Spain.

Oteri, A.U., 1981. Geoelectric investigation of saline contamination of chalk aquifer by mine drainage water at Tilmanstone, England. Geoexploration, 19: 179-192.

Paranjape, S.C., 2009. Groundwater information, Sindhudurg district, Maharashtra. Technical Report 1625/DB/2009, Central Ground Water Board, India.

Powar, K.B., 1993. Geomorphological evolution of Konkan coastal belt and adjoining Sahyadri uplands with reference to Quarternary uplift. Curr. Sci., 64: 793-796.

Sarkar, P.K., and Soman, G.R., 1983. Geological and quantitative geomorphological studies of the coastal Golvan basin, north of Malvan, Sindhudurg district, Maharashtra. Prof. Kelkar Mem. Volume, Ind. Soc. Earth Sci., 157-172.

Sarkar, P.K., and Soman, G.R., 1986. Geology of the area around Katta, Sindhudurg district, Maharashtra, based on aerospace data. Photonirvachak, 14(2): 43-51.

Song, S.H., Lee, J.Y., and Park, N., 2007. Use of vertical electrical soundings to delineate seawater intrusion in a coastal area of Byunsan, Korea. Environ. Geol., 52: 1207-1219.

Srinivas, Y, Hudson Oliver, D., Stanley Raj, A., and Chandrasekar, N., 2014. Delineation of groundwater potential zones along the coastal parts of Kanyakumari district, Tamilnadu. Jour. Ind. Geophys. Union, 18(3): 356-362.

Todd, D.K., 1980. *Groundwater Hydrology*, In: 2nd Ed. Wiley India, 431-457.

Verma, R.K., Rao, M.K., and Rao, C.V., 1980. Resistivity investigations for ground water in metamorphic areas near Dhanbad, India. Ground Water, 18(1): 46–55.

Vijay Kumar, D., Ramadass, G., and Jagadish, S.V., 2015. Delineation of Groundwater Potential Zones through Electrical Resistivity Parameters in hard rock terrain, Osmania University Campus, Hyderabad, Telangana State, India. IOSR Journal of Applied Geology and Geophysics, 3(6): 1-10.

Webster, R., and Oliver, M.A., 2001. Geostatics for environmental scientists. Wiley, Chichester.

Zohdy, A.A.R., Eaton, G.P., and Mabey, D.R., 1974. Application of surface geophysics to ground-water investigation. In: 2nd ed United States Geological Survey, USA.